

edges, and that it is quite different from crystal to crystal are all consistent with the need to overcome the effects of strain fields before the magnetic field is effective in determining which  $\mathbf{Q}$  is preferred. In this model we have presumed that the energy to create walls between regions of different  $\mathbf{Q}$  vectors is much larger than that for creation of polarization walls within "single- $\mathbf{Q}$ " regions. We note in this connection that in a field of 12 kG there is no difference in the volumes associated with each  $\mathbf{Q}$  for a "multi- $\mathbf{Q}$ " crystal, and

that applying and removing a 30-kG field produced no change in a "single- $\mathbf{Q}$ " crystal when the field was applied perpendicular to  $\mathbf{Q}$ . With this model we would expect the crystals to be more likely "single- $\mathbf{Q}$ " the greater their freedom from inhomogeneous strain. This is in agreement with the findings of Graebner and Marcus who found that the vapor-grown crystals with the highest ratio of room temperature to residual resistivity were the most likely to be anisotropic when cooled in zero field.

## Paraelectric-Ferroelectric Phase Boundaries in Semiconducting Perovskite-Type Crystals

M. DiDOMENICO, JR., AND S. H. WEMPLE

*Bell Telephone Laboratories, Murray Hill, New Jersey*

(Received 26 October 1966)

The formation of first-order paraelectric-ferroelectric phase boundaries in semiconducting crystals of the ferroelectrics  $\text{KTa}_{0.65}\text{Nb}_{0.35}\text{O}_3$  and  $\text{BaTiO}_3$  has been studied. It is shown that in crystals having carrier concentrations greater than  $10^{16} \text{ cm}^{-3}$ , sharp first-order phase boundaries can form during the paraelectric-ferroelectric phase transformation, and that such a transformation results in the formation of reproducible single-domain crystals. The direction of the cubic-to-tetragonal phase boundary is found to differ from a  $\{110\}$  lattice plane by approximately  $5^\circ$ , i.e., the boundary-plane normal is  $40^\circ$  from the direction of the crystal  $c$  axis. This result is in excellent agreement with existing crystallographic theories. Data are also presented on the infrared photo-ionization absorption anisotropy and the electrical resistance anisotropy measured on a single-domain semiconducting crystal of  $\text{KTa}_{0.65}\text{Nb}_{0.35}\text{O}_3$ .

### INTRODUCTION

IT has been well established that an insulating ferroelectric crystal, when cooled through one of its transition temperatures, undergoes a metastable nucleation process that results in a variety of possible multiple-domain configurations which are generally nonreproducible. In semiconducting ferroelectric crystals, on the other hand, the situation should be quite different because the free charges present can compensate, or neutralize, the bound polarization charges inside the crystal thereby making possible the formation of reproducible single-domain crystals. We have observed, for example, that upon cooling a thin rectangular slab of the semiconducting ferroelectric  $\text{KTa}_{0.65}\text{Nb}_{0.35}\text{O}_3$  (hereafter abbreviated KTN) through its cubic-tetragonal phase transition a sharply defined boundary forms dividing the crystal into a paraelectric (cubic) and a ferroelectric (tetragonal) phase. This first-order phase boundary or habit plane moves from one end of the crystal to the other during the phase transformation leaving behind a single domain ferroelectric crystal.

Such diffusionless phase boundaries in partially transformed single crystals are well known in metallurgy and have been studied extensively in a number of metal alloys, most notably the austenite-martensite transfor-

mation in steel.<sup>1-4</sup> Wechsler, Lieberman, and Read<sup>2</sup> (WRL) have shown theoretically that, when certain assumptions are made as to the detailed nature of the slip and/or twinning system, the direction of the habit-plane normal can be determined from a knowledge of the lattice parameters of the initial and final phases. Based largely on theoretical predictions, it was in fact suggested<sup>4</sup> some time ago that the WLR theory should be applicable to perovskite-type ferroelectric crystals. We believe that the results presented here give unambiguous experimental evidence for habit plane formation in these materials and that these results are quantitatively explainable in terms of the WLR crystallographic theory. It should be emphasized that such crystallographically determined boundaries are permitted only in semiconducting ferroelectrics where there is sufficient free charge available to provide a termination for the spontaneous polarization at the paraelectric-ferroelectric interface.

<sup>1</sup> See, for instance, J. W. Christian, *The Theory of Transformations in Metals and Alloys* (Pergamon Press, Inc., New York, 1965).

<sup>2</sup> M. S. Wechsler, D. S. Lieberman, and T. A. Read, *Trans. AIME* **197**, 1503 (1953).

<sup>3</sup> M. W. Burkart and T. A. Read, *Trans. AIME* **197**, 1516 (1953).

<sup>4</sup> D. S. Lieberman, M. S. Wechsler, and T. A. Read, *J. Appl. Phys.* **26**, 473 (1955).

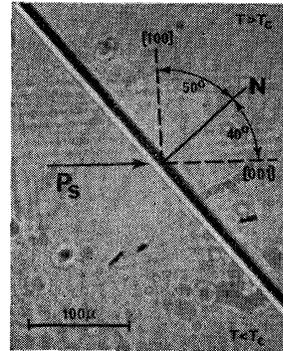
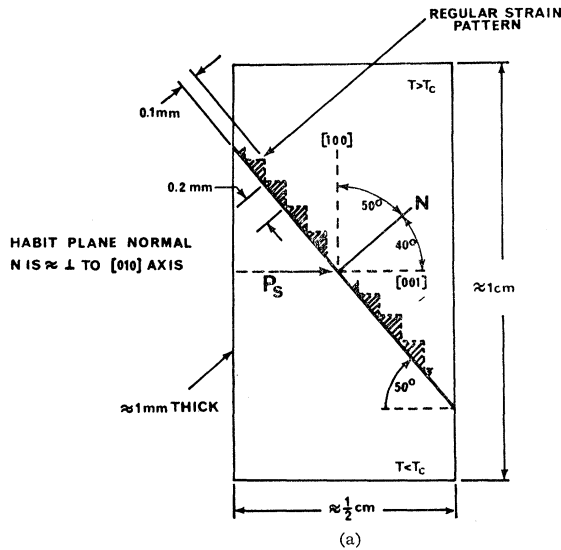


FIG. 1. (a) Schematic drawing summarizing overall observed characteristics of paraelectric-ferroelectric phase boundaries in semiconducting KTN. (b) Photomicrograph of phase boundary in KTN taken in polarized light. The tetragonal region (bottom half) has spontaneous polarization  $P_s$  in the direction indicated.

In this paper we report the results of an investigation on the formation of cubic to tetragonal phase boundaries in semiconducting crystals of KTN and BaTiO<sub>3</sub>. The observations are compared with the WLR theory which predicts that the habit plane is close to a {110} lattice plane; exact values are quoted below. It is shown that the measured and calculated directions of the habit-plane normal are in excellent agreement. Some comments are also offered concerning possible strain relief mechanisms at the interface and the influence of the free charge sheet present at the interface. Because the product of the phase transformation is a single domain ferroelectric crystal, it is possible to measure the effects of the phase transformation on electrical and optical properties. We report briefly on the electrical resistivity and infrared absorption anisotropies in single-domain ferroelectric KTN.

### PROPERTIES OF KTN

The mixed crystal KTN is a solid solution of the perovskite oxides KTaO<sub>3</sub> and KNbO<sub>3</sub> in the ratio 0.65/0.35. The dielectric properties of insulating KTN have been reported elsewhere.<sup>5</sup> KTN exhibits a first-order cubic-tetragonal phase transition, or Curie point, at  $T_c \approx 10^\circ\text{C}$  with a spontaneous polarization of nearly  $5 \mu\text{C}/\text{cm}^2$ . In crystals having a niobium to tantalum ratio less than approximately 0.4, the transition becomes second order. Above the Curie point, KTN has the ideal cubic perovskite structure with a lattice constant of  $a_0 = 3.988 \text{ \AA}$ .<sup>6</sup> Below the Curie point, the crystals become tetragonal with a spontaneous strain (extension) along the crystalline  $c$  axis of

$$\Delta c/c \approx 4.5 \times 10^{-6} P_s^2, \quad (1)$$

where  $P_s$  is the spontaneous polarization expressed in  $\mu\text{C}/\text{cm}^2$ . In the  $a$  direction, normal to the  $c$  axis, the crystal contracts by an amount

$$\Delta a \approx 0.42 \Delta c. \quad (2)$$

Under certain growth conditions, KTN crystals become extrinsic  $n$ -type semiconductors in which the donors are probably associated with oxygen vacancies. Conduction in these crystals is thought to occur in  $d$  bands formed from Nb(4d) and Ta(5d) orbitals. Theoretical calculations<sup>7</sup> indicate that the lowest conduction band is many-valleyed with the valley minima occurring at the zone boundary in  $\langle 100 \rangle$  directions. The band gap determined optically is 3.4 eV; the donors are approximately 0.2–0.3 eV below the conduction band. The semiconducting crystals exhibit resistivities in the 1–10  $\Omega \text{ cm}$  range and appear blue in color due to donor photoionization and free-carrier absorption. Hall measurements give a room temperature Hall mobility of 3.3  $\text{cm}^2/\text{V sec}$ . The ratio of conductivity effective mass to free electron mass is about 1.5. For a more extensive discussion of the transport properties of some other perovskite-type oxides the reader is referred to the literature.<sup>8,9</sup>

### EXPERIMENTAL

Observations of the cubic to tetragonal phase transformation in semiconducting KTN at  $10^\circ\text{C}$  were made visually with a polarizing microscope equipped with a CO<sub>2</sub> gas-operated microcold stage. Figure 1(a) illustrates the salient features of the over-all observations, while Fig. 1(b) shows in detail a boundary photo-

<sup>7</sup> A. H. Kahn and A. J. Leyendecker, Phys. Rev. **135**, A1321 (1964).

<sup>8</sup> S. H. Wemple, Phys. Rev. **137**, A1575 (1965).

<sup>9</sup> H. P. R. Frederikse, W. R. Thurber, and W. R. Hosler, Phys. Rev. **134**, A442 (1964).

<sup>5</sup> F. S. Chen, J. E. Geusic, S. K. Kurtz, J. G. Skinner, and S. H. Wemple, J. Appl. Phys. **37**, 388 (1966).

<sup>6</sup> V. T. Murphy and M. C. Huffstutler, Jr. (private communication).

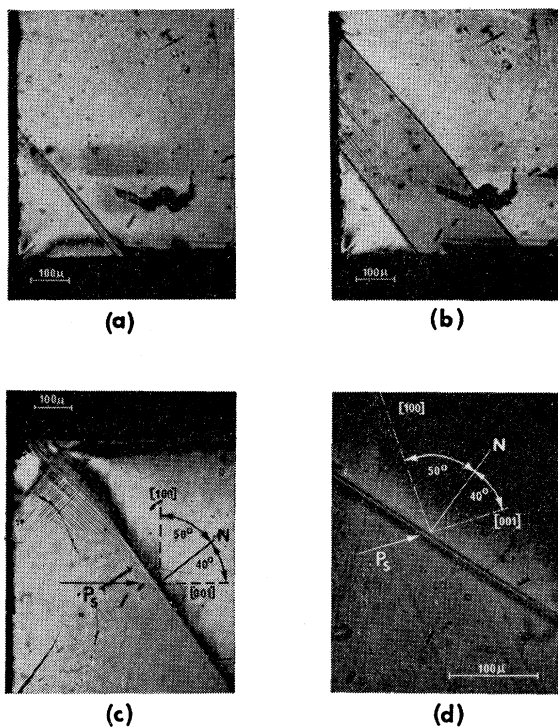


FIG. 2. Photomicrographs of KTN taken in analyzed light showing growth of ferroelectric spike in (a) and (b), and strain relief pattern on paraelectric side of phase boundary in (c) and (d).  $P_s$  is the direction of spontaneous polarization.

graphed at high magnification. Boundaries of the kind shown in Fig. 1 occur only in high-quality single crystals. Under carefully controlled thermal conditions a stable boundary will form. Any small thermal fluctuations, however, such as produced from a small microscope lamp, will cause the boundary to move reversibly.

The crystals chosen for investigation were as large as  $1 \text{ cm} \times \frac{1}{2} \text{ cm} \times 1 \text{ mm}$  thick but were more typically in the range of about  $\frac{1}{2} \text{ cm}$  in cross section by  $\frac{1}{2} \text{ mm}$  thick. The habit-plane normal  $N$  was found to be  $40 \pm 1^\circ$  from the  $c$  axis or direction of spontaneous polarization, and was perpendicular to the  $[010]$  axis to within less than  $1^\circ$  [see Fig. 1(a)]. These results are in excellent agreement with the crystallographic theory described below. Along the habit plane a regular strain pattern was observed in the paraelectric phase as shown schematically in Fig. 1(a). This pattern, observed with the crystal between crossed polarizers, had an average spatial period along the boundary interface of about 0.2 mm and extended an average distance of about 0.1 mm into the paraelectric phase. The photograph shown in Fig. 1(b) was taken in light polarized parallel to the habit plane and shows the sharpness of the habit plane interface. It is believed that the boundary photographs as a thick  $\approx 10\text{-}\mu$ -wide line because of free-carrier absorption in the polarization-neutralizing charge sheet present at the interface.

In Fig. 2, photomicrographs taken under various

thermal conditions in different parts of a high-quality KTN sample are shown. Figures 2(a) and (b) show how one particular crystal goes through the transition. In Fig. 2(a) we show a ferroelectric spike nucleating just at the Curie temperature of  $10.5^\circ\text{C}$  in one corner of the crystal. At a slightly lower temperature, the spike grows into a band as shown in Fig. 2(b). Further small reductions in temperature cause the band to expand such that the crystal divides into two partly transformed regions, one ferroelectric and the other paraelectric, as indicated schematically in Fig. 1(a). Figures 2(c) and 2(d) are photographs showing the regular strain-relief pattern at the boundary observed under low and high magnification, respectively. These photographs, which were taken in analyzed light, show the spatial periodicity of the strain pattern [Fig. 2(c)] and some of the detail in a single period [Fig. 2(d)]. As shown in Fig. 2(d), the edges of the strain pattern are aligned with respect to the crystal  $\langle 100 \rangle$  axes in the cubic phase. It should be noticed also that the length to width aspect ratio of a single period of the strain pattern is approximately 2.

The  $c$  axis and direction of spontaneous polarization shown in Figs. 1 and 2 were determined experimentally from optical and pyroelectric observations. Using the fact that the crystal is negative uniaxial in the ferroelectric phase, the tetragonal or  $c$  axis was uniquely determined by conventional optical techniques using a Soleil-Babinet compensator. The direction of spontaneous polarization within the crystal was established by measuring the direction of pyroelectric current flow<sup>10</sup> on heating the crystal. The  $c$  axis determined in this way agreed with the optical measurements. From the pyroelectric measurements the *direction* of the spontaneous polarization was such that the positive end of the dipole-chain terminated at the phase boundary thereby creating a compensating electron accumulation charge sheet. In a few cases boundaries were observed to form between tetragonal phases having opposite directions of spontaneous polarization.

Habit-plane boundaries have also been observed in crystals of semiconducting  $\text{BaTiO}_3$  doped with cerium. The direction of the habit-plane normal with respect to the  $c$  axis of the crystal was found to be almost identical to that in KTN (i.e.,  $40^\circ$ ). This result is in agreement with the crystallographic theory described below. Further, a strain-relief pattern similar to that shown in Fig. 1(a) was observed in the paraelectric phase. Sharp habit-plane boundaries have been observed previously in  $\text{BaTiO}_3$  by other workers<sup>11,12</sup> although no explanation was given as to the nature of their formation or to their ability to be reproduced. This is to be contrasted with

<sup>10</sup> A. G. Chynoweth, J. Appl. Phys. **27**, 78 (1956).

<sup>11</sup> D. Meyerhofer, Phys. Rev. **112**, 413 (1958).

<sup>12</sup> T. J. Parker and J. C. Burfoot, Brit. J. Appl. Phys. **17**, 207 (1966); J. C. Burfoot and T. J. Parker, *ibid.* **17**, 213 (1966).

the reproducible observations reported here on KTN and BaTiO<sub>3</sub> crystals having resistivities in the 1–10 Ω cm range.

### CRYSTALLOGRAPHIC THEORY

We have previously alluded to the fact that the habit plane normal  $\mathbf{N}$  can be calculated according to the WLR theory from a specification of the slip and/or twinning system and the lattice parameters of the initial and final phases. The purpose of this section is to outline some of the physical reasoning which is central to the crystallographic theory developed by other workers,<sup>2-4</sup> and to quote the formula for the direction of the habit-plane normal. The particular problem of concern is to understand how a cubic structure (paraelectric phase) transforms into a tetragonal structure (ferroelectric phase).

Briefly, the physical formation of the habit plane can be understood using the following arguments. We note that we are concerned with coherent interfaces and that generally this kind of interface cannot form between two single crystals without producing severe elastic strain over appreciable distances owing to the lattice-matching process. According to St. Venant's principle,<sup>13</sup> the strain would have to extend over a distance comparable to the linear dimension of the cross section of the crystal or in our case typically about  $\frac{1}{2}$  cm. To reduce this misfit strain energy to a minimum it is necessary that the lower symmetry crystal phase be twinned so that the sign of the strain reverses in going from one twin to the next along the habit plane. This then defines a plane of zero average distortion.<sup>2</sup> The total strain energy stored at the interface can be estimated as follows. The energy is divided into two parts. The first is the strain energy at the interface, and the second is the twin-surface wall energy. It is easy to show<sup>3,4</sup> that the sum of these energies is minimized when the twin surface energy equals the strain energy. Making use of this result, we estimate that the minimum total strain energy per unit area stored at the interface is of the order

$$W \sim \bar{c}\epsilon^2 t, \quad (3)$$

where  $\bar{c}$  is an average elastic modulus,  $\epsilon$  the strain, and  $t$  the twin thickness. For KTN,  $\bar{c} \approx 2 \times 10^{12}$  dyn/cm<sup>2</sup>, from Eq. (1) using  $P_s = 5$  μC/cm<sup>2</sup>  $\epsilon \approx 1.3 \times 10^{-4}$ , and from Fig. 1(a) the maximum twin thickness determined by St. Venant's principle is  $t \lesssim 100$  μ. Therefore we estimate that an upper limit to the strain energy is  $W \sim 300$  ergs/cm<sup>2</sup>, but that it could be as low as  $W \sim 30$  ergs/cm<sup>2</sup> if the twin thickness were as small as 10 μ. Actually, this is the electrostrictive strain energy per unit area associated with the spontaneous lattice strain in a twin thickness, and it is believed to be comparable to the actual misfit strain energy. It is important to ask how

this compares with the electrical energy stored in the boundary. Order-of-magnitude calculations made by Berglund<sup>14</sup> using thermodynamic considerations suggest that the electrical energy stored in the boundary is between 0.1–10 ergs/cm<sup>2</sup> depending on the carrier concentration. The highest estimate corresponds to a carrier concentration  $n$  of about  $10^{16}$  cm<sup>-3</sup> and the lowest to a concentration of about  $10^{18}$  cm<sup>-3</sup>. Based on these results and the fact that in our samples  $n \approx 10^{17}$ – $10^{18}$  cm<sup>-3</sup>, it is reasonable to expect that the formation of the habit plane will be governed primarily by interfacial strain energy and crystal-matching considerations.

It has been shown<sup>2</sup> that the requirement that the habit plane be one of zero average distortion defines a crystallographic problem with a unique mathematical solution. The result obtained by WRL is that the direction cosines  $(h, k, l)$  of the habit plane normal  $\mathbf{N}$  are given by

$$h = \frac{1}{2\eta_1} \left[ \left( \frac{2\eta_1^2\eta_2^2 - \eta_1^2 - \eta_2^2}{\eta_2^2 - 1} \right)^{1/2} - \left( \frac{\eta_1^2 + \eta_2^2 - 2}{\eta_2^2 - 1} \right)^{1/2} \right], \quad (4)$$

$$k = \frac{1}{2\eta_1} \left[ \left( \frac{2\eta_1^2\eta_2^2 - \eta_1^2 - \eta_2^2}{\eta_2^2 - 1} \right)^{1/2} + \left( \frac{\eta_1^2 + \eta_2^2 - 2}{\eta_2^2 - 1} \right)^{1/2} \right], \quad (5)$$

$$l = \frac{1}{\eta_1} \left( \frac{1 - \eta_1^2}{\eta_2^2 - 1} \right)^{1/2}, \quad (6)$$

in which  $\eta_1$  and  $\eta_2$  are dimensionless parameters called the principal distortions defined as  $\eta_1 = a/a_0$  and  $\eta_2 = c/a_0$ . With these definitions and Eq. (2) we obtain for KTN

$$\eta_1 = 1 - 0.42\Delta c/a_0, \quad (7)$$

and

$$\eta_2 = 1 + \Delta c/a_0. \quad (8)$$

Substituting Eq. (1) with  $c \approx a_0$  into Eqs. (7) and (8) and then substituting these results into Eqs. (4), (5), and (6) gives to a very good approximation

$$h \approx 0, \quad k \approx 0.76, \quad l \approx 0.65.$$

The solution for the habit plane indices  $(h, k, l)$  does not uniquely define the orientation of the habit plane since symmetry allows a multiplicity of up to 24 crystallographically equivalent solutions. The angles of the habit-plane normal  $\mathbf{N}$  are defined with respect to the crystallographic axes of the parent cubic phase and are 90°, 49.7° and 40.3°. These values are in excellent agreement with the measured angles 89–90°, 50 ± 1°, and 40 ± 1°. As indicated by these angles and also by the form of Eqs. (4), (5), and (6), the habit plane is irrational deviating by approximately 5° from a {110} lattice plane in KTN and BaTiO<sub>3</sub>.

It has been mentioned that the symmetry loss in the ferroelectric phase results in a multiplicity of possible tetragonal structures. It has also been mentioned that

<sup>13</sup> G. Nadeau, *Introduction to Elasticity* (Holt, Rinehart, and Winston, Inc., New York, 1964).

<sup>14</sup> C. N. Berglund (unpublished results).

in order to establish the habit plane as a plane of zero average distortion a twinned structure is necessary. Both of these conditions result in the formation of a banded tetragonal twin structure or domain structure along the habit plane. The relative amounts of the two twins (domains)  $X$  and  $1-X$  can be found from the following equation derived by WLR:

$$X = \frac{1}{2} \pm \frac{1}{2} [(1 - \eta_1^2 \eta_2^2) / (\eta_1^2 - \eta_2^2)] (1 - A^2)^{1/2}, \quad (9)$$

where

$$A = (\eta_1^2 - 1)(1 - \eta_2^2) / (1 - \eta_1^2 \eta_2^2).$$

For KTN  $X$  is very close to  $\frac{1}{3}$ . As a consequence, we expect that in the ferroelectric phase a sandwiched structure of alternating  $a$  domains and  $c$  domains should extend along the habit plane. To balance out strains along the habit plane, Eqs. (1), (2), and (9) indicate that the  $a$  domains with the direction of spontaneous polarization pointing into the habit plane should be very nearly twice as wide as the  $c$  domains. The absolute twin or domain width should be between  $10 \mu$  and  $100 \mu$  based on the observations summarized in Fig. 1(a). Simple lattice matching arguments would favor the  $10 \mu$  domain width. Below the habit plane and well into the ferroelectric phase a single  $a$  domain may be observed. A structure very similar to this has been described and schematically pictured by Burkart and Read<sup>3</sup> in an indium-thallium alloy single crystal. We point out that the banded twin structure was not observed in the ferroelectric phase with a polarizing microscope. However, what we believe to be the effect of this structure, that is, the regular strain pattern in the paraelectric phase has been observed.

### DISCUSSION

As shown in the preceding section, the direction of the habit plane normal at the paraelectric-ferroelectric interface in semiconducting KTN is in excellent agreement with existing crystallographic theories. It is easy to show from Eqs. (4)–(8) that the habit plane direction is determined essentially by the ratio  $\Delta a / \Delta c$  [e.g.,  $l \approx (\Delta a / \Delta c)^{1/2}$ ] for small deviations from cubic symmetry. Since this ratio is nearly the same in a variety of perovskite ferroelectrics, very similar results to those reported here for KTN are expected in other semiconducting perovskites. The observed direction of the habit plane normal in semiconducting BaTiO<sub>3</sub> is in agreement with this conclusion.

It was pointed out earlier that high quality semiconducting crystals of KTN transform quite readily into single domain ferroelectric crystals below their Curie point. The reason for this is that the free charges present in conducting crystals neutralize the bound polarization charge inside the crystal. The situation is quite different, however, in highly insulating crystals since in this case the absence of free charges imposes the restriction that phase boundaries be free of any excess

polarization charge. Formation of the ferroelectric phase then involves nucleation and growth of narrow ferroelectric spikes resulting generally in a nonreproducible multi-domain configuration comprised largely of so-called  $90^\circ$  domains.<sup>15</sup> These domains allow the polarization to change direction by  $90^\circ$  without accumulating any excess charge. Under special conditions in high-quality crystals it may be possible for a particular spike to grow to sufficient size to give fairly large single domain sections of crystal. However, these sections are usually very unstable to any kind of stress perturbation.

It is of interest to estimate the free charge density  $\rho_f$  required to insure single domain formation in semiconducting ferroelectrics. The bound polarization charge density  $\rho_b$  is related to the crystal polarization  $\mathbf{P}$  by

$$\nabla \cdot \mathbf{P} = -\rho_b. \quad (10)$$

For the sake of simplicity, we take a one-dimensional model in which the polarization goes from its saturated value  $P_s$  in the bulk of the ferroelectric phase to zero at the habit plane on the paraelectric side in a characteristic length  $\lambda$ . Equation (10) then gives

$$\rho_b \approx P_s / \lambda. \quad (11)$$

If the free charge density  $\rho_f$  is equal to or greater than this value, there exists sufficient neutralizing charge for a single domain to form. If, on the other hand,  $\rho_f$  is less than  $\rho_b$ , the excess polarization charges induced on the surface of the crystal will create depolarizing fields which make it energetically less desirable to have a single domain.<sup>16</sup> We therefore expect to form a single-domain crystal when

$$\rho_f > P_s / \lambda. \quad (12)$$

Experimentally we determine from Fig. 1(b) that a reasonable estimate for  $\lambda$  is  $\approx 10 \mu$ . Substituting this value into Eq. (12) together with  $P_s = 5 \mu\text{C}/\text{cm}^2$ , we conclude that the free-carrier density  $n$  necessary to form a single domain crystal is of the order  $n > 10^{16} \text{ cm}^{-3}$ . This is consistent with the carrier concentrations of the KTN and BaTiO<sub>3</sub> crystals used in the experimental work which were typically in the range  $10^{17}$ – $10^{18} \text{ cm}^{-3}$ .

Estimates<sup>14</sup> of the electrical energy stored in paraelectric-ferroelectric phase boundaries suggest a rapid increase of energy with decreasing free-charge density. These order-of-magnitude estimates of the electrical stored energy imply that in the more insulating crystals of KTN, having carrier concentrations below  $10^{16} \text{ cm}^{-3}$  or resistivities above  $1000 \Omega \text{ cm}$ , the electrical energy will be comparable to or larger than the stored strain energy. Accordingly, a multiple domain configuration and a habit plane determined by electrical energy considerations will prevail.

<sup>15</sup> E. A. Little, Phys. Rev. **98**, 978 (1955).

<sup>16</sup> F. Jona and G. Shirane, *Ferroelectric Crystals* (The Macmillan Company, New York, 1962), p. 45.

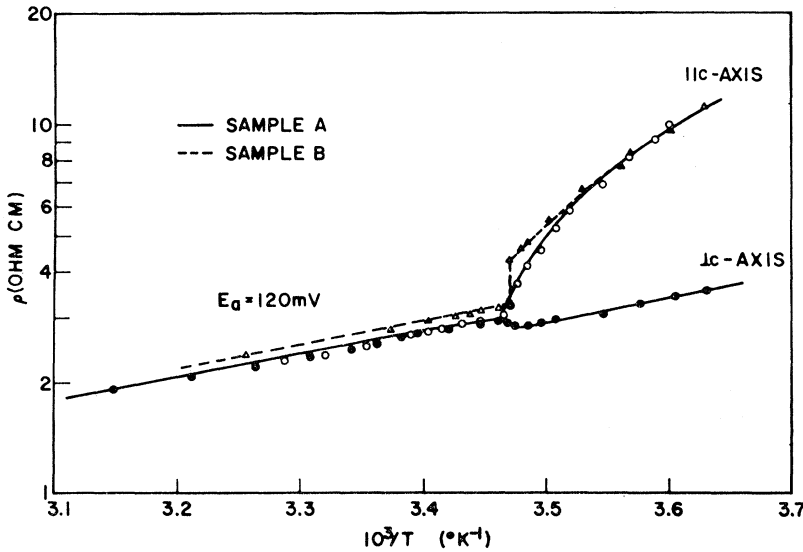


FIG. 3. Temperature dependence of electrical resistivity  $\rho$  in KTN observed perpendicular and parallel to the crystal  $c$  axis. The lack of a clearly defined discontinuity at  $T_c \approx 15^\circ\text{C}$  in sample A is attributed to crystalline inhomogeneities which tend to smear out the transition. A sharply defined transition is evident in sample B, however.

This discussion leaves unanswered how the polarization varies spatially within the phase-boundary region. This problem is complicated by the interaction between the semiconducting and ferroelectric properties of the crystal in the vicinity of the boundary plane. To single out one important interaction consider how the conduction band structure is modified by the ferroelectricity in this region. The shearing strains near the boundary will rotate the polarization to some extent and

introduce a deformation-potential correction to the energy of the conduction band. In addition, the accumulation of free carriers needed to neutralize the divergence of crystal polarization will introduce a macroscopic potential which will also act to depress the conduction band energy. The detailed balance between the changing direction and magnitude of the polarization with the concomitant changes in the band structure will clearly result in establishing an equilibrium which will deter-

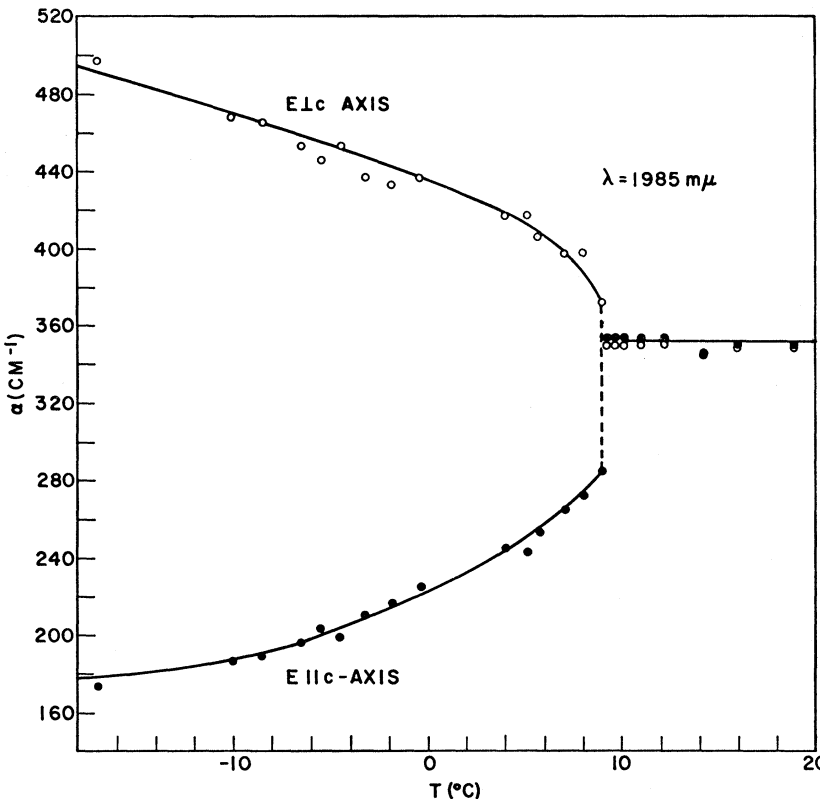


FIG. 4. Optical absorption coefficient  $\alpha$  as a function of temperature in KTN at  $\lambda = 1985 \text{ m}\mu$  for light polarized perpendicular to  $(E \perp c)$  and parallel to  $(E \parallel c)$  the crystal  $c$  axis.

mine the precise properties of the polarization in the neighborhood of the boundary plane. Consistent with the approximations made in this paper we neglect the effect of the semiconducting properties on the behavior of the polarization and assume that the polarization follows closely the deformation of the lattice as determined crystallographically.

A significant advantage in being able to produce large single domain ferroelectric crystals, as well as sharp paraelectric-ferroelectric phase boundaries, is that one can readily study transport, optical, dielectric, and elastic properties both above and below the Curie point in unpoled crystals. We show, for example, in Figs. 3 and 4, the resistance anisotropy and infrared dichroism measured as a function of temperature on two high-quality KTN crystals. Above the Curie point where the crystals are cubic both properties are isotropic. The resistivity data of Fig. 3 obtained using a four-terminal method show that the resistance increases parallel to the polarization or  $c$  axis and decreases slightly in the perpendicular direction. The activation energy above  $T_c$ ,  $E_a \approx 120$  mV, corresponds to donors situated ap-

proximately 0.24 eV below the conduction band edge. The optical data of Fig. 4 were obtained at a wavelength of  $1.985 \mu$  corresponding to the peak in the near infrared donor photo-ionization absorption. These data show a discontinuous first-order change in the absorption coefficient at the Curie point. In the ferroelectric phase the absorption is greater for light polarized perpendicular to the crystal  $c$  axis ( $E \perp c$ ). Results of a complete study of transport and optical properties of KTN in the vicinity of the Curie point will be reported in the near future.

#### ACKNOWLEDGMENTS

The authors thank I. Camlibel and E. F. Kankowski for their assistance with some of the experimental work. Thanks are also extended to W. A. Bonner and L. G. Van Uitert for generously supplying the KTN crystals, and A. Linz of MIT for providing the BaTiO<sub>3</sub> crystals. Finally we are grateful to Professor D. S. Lieberman and to the late Professor T. A. Read of the University of Illinois for critically reading the manuscript and for helpful discussions.

### Ising-Model Critical Indices below the Critical Temperature\*

GEORGE A. BAKER, JR.

*Applied Mathematics Department, Brookhaven National Laboratory, Upton, New York and*

*Wheatstone Physics Laboratory, King's College, University of London, London, England*

AND

DAVID S. GAUNT

*Wheatstone Physics Laboratory, King's College, University of London, London, England*

(Received 20 October 1966)

We review the estimates for the critical indices of the Ising model below  $T_C$  and conclude (for 3 dimensions):  $\alpha' = 0.066_{-0.04}^{+0.16}$ ,  $\beta = 0.312_{-0.005}^{+0.002}$ ,  $\gamma' = 1.310_{-0.05}^{+0.04}$  for the specific heat, magnetization, and magnetic susceptibility, respectively. For 2 dimensions, we estimate  $\gamma' = 1.75_{-0.00}^{+0.01}$ . In order to explain previous estimates of  $\alpha' = 0$ , we point out that a low power can, in practice, look deceptively like a logarithm. Finally, we discuss the behavior of the specific heat at constant magnetization.

#### 1. INTRODUCTION AND SUMMARY

IN recent years, various workers have estimated from power-series expansions the various critical indices for the two- and three-dimensional Ising model. In 1963 it was speculated<sup>1</sup> that a certain relation must hold between three of the critical indices below the critical point. Later that year, this conjectured equality was proved as a rigorous inequality.<sup>2</sup> Unfortunately, the best available estimates at that time failed, by 6¼%, to

satisfy this relation for the three-dimensional Ising model, although they satisfied it for the two-dimensional model. It is the purpose of this paper to critically re-examine the various estimates, to attempt to establish realistic error bounds on them, and to reconcile them with all available information.

We conclude from our study that  $C_M/C_H$  is probably continuous at  $T_c$  for the three-dimensional Ising model and that it is continuous for the two-dimensional model. As a consequence

$$2 \leq \alpha' + 2\beta + \gamma' < 2 + \epsilon, \quad (1.1)$$

where  $\epsilon \sim 0.1$  for three dimensions and 0.01 for two

\* Part of this work performed under the auspices of the U. S. Atomic Energy Commission.

<sup>1</sup> J. W. Essam and M. E. Fisher, *J. Chem. Phys.* **38**, 802 (1963).

<sup>2</sup> G. S. Rushbrooke, *J. Chem. Phys.* **39**, 842 (1963).

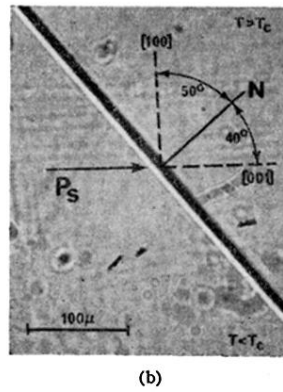
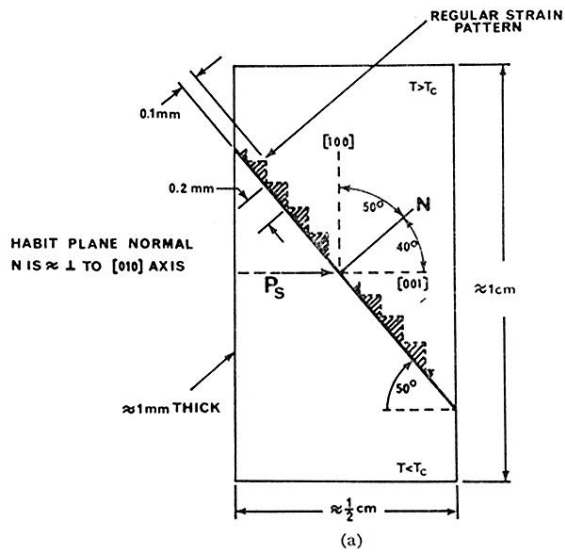


FIG. 1. (a) Schematic drawing summarizing overall observed characteristics of paraelectric-ferroelectric phase boundaries in semi-conducting KTN. (b) Photomicrograph of phase boundary in KTN taken in polarized light. The tetragonal region (bottom half) has spontaneous polarization  $P_s$  in the direction indicated.

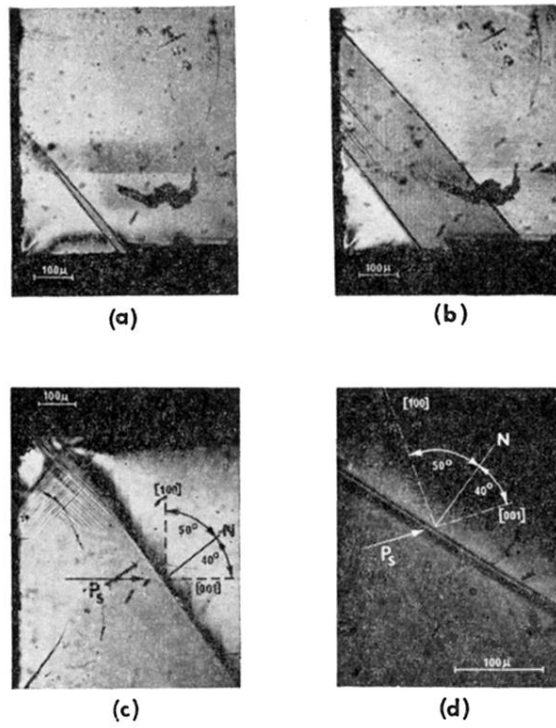


FIG. 2. Photomicrographs of KTN taken in analyzed light showing growth of ferroelectric spike in (a) and (b), and strain relief pattern on paraelectric side of phase boundary in (c) and (d).  $P_s$  is the direction of spontaneous polarization.